Clusters, Liquids, and Crystals of Dialkyimidazolium Salts. A Combined Perspective from ab Initio and Classical Computer Simulations

MARIO G. DEL PÓPOLO,*,† JORGE KOHANOFF,†
RUTH M. LYNDEN-BELL,†,‡ AND
CARLOS PINILLA†

Atomistic Simulation Centre, School of Mathematics and Physics, Queen's University Belfast, Belfast BT7 1NN, U.K., and University Chemical Laboratory, Lensfield Road, Cambridge University, Cambridge CB2 1EW, U.K.

Received March 19, 2007

FIGURE 1. 1-Alkyl-3-methyl imidazolium cation. In this case, the alkyl chain in position 1 is a butyl group.

ABSTRACT
We summarize results obtained by a combination of ab initio and classical computer simulations of dialkylimidazolium ionic liquids in different states of aggregation, from crystals to liquids and clusters. Unusual features arising from the competition between electrostatic, dispersion, and hydrogen-bonding interactions are identified at the origin of observed structural patterns. We also discuss the way Brønsted acids interact with ionic liquids leading to the formation of hydrogen-bonded anions.

I. Introduction

Room-temperature ionic liquids (RTILs) are in many ways similar to the more familiar inorganic molten salts. They share the common feature of being made of charged particles bound largely by electrostatic interactions. RTILs, however, are richer in many respects. Their large organic

cations sustain enhanced dispersion interactions and can also be involved in hydrogen bonding. Since almost a decade ago, it has become increasingly clear that differences in the physicochemical properties of these two classes of systems have to be rationalized from a microscopic point of view.

In this Account, we summarize some lessons learned from classical and ab initio simulations of alkylimidazolium salts (see Figure 1). As a first topic, we discuss the behavior of RTILs when restricted to form small aggregates.[1] The interest on RTIL clusters stems from the possibility of investigating the evolution of properties and phenomena with system size such as the precursors of phase transitions observed in the bulk, the size dependence of dielectric and dynamical properties, the relative contribution of Coulomb and van der Waals interactions to cohesion, and the stability of charged nanodroplets. Some of these topics can be examined experimentally in electrosprays[2] or with modern beam techniques.[3] Furthermore, the recent experimental demonstration that RTILs possess a thin but detectable vapor phase[4] routes the attention toward the small aggregates present in the vapor.

Electronic density functional theory (DFT) is one of the tools of the trade in computational material science providing a unified description of covalent, ionic, and hydrogen bonding, including electronic polarization. Here we compare the liquid structure of a model RTIL calculated from first-principle simulations with that measured in neutron diffraction experiments or simulated with empirical potentials.[5] Moderate hydrogen bonding between cation and anion appears as the cause of important structural motifs in both the liquid and the solid phase of this model salt. Furthermore, the electrostatic properties of the ions are examined by analyzing the electronic wave functions over a sample of configurations.[6]

Nowadays it is well recognized that the most popular DFT schemes, based on local (LDA) and semilocal (for example, Perdew–Burke–Ernzerhof generalized gradient approximation, PBE-GGA) approximations to the exchange and correlation functional, do not contain the necessary ingredients to describe dispersion interactions.[7,8]

Mario Del Pópolo received his Ph.D. in Chemistry from the National University of Córdoba, Argentina, in 2002. After a year of postdoctoral work at the Henry Eyring Centre for Theoretical Chemistry (University of Utah), he joined the Atomistic Simulation Centre at Queen's University Belfast, where he holds an academic position since 2006. His research interests focus on the statistical mechanics and computer simulation of condensed phase systems, with emphasis on complex fluids and chemical reactivity.

Jorge Kohanoff graduated from the University of Buenos Aires (Argentina) in 1986 and obtained an M.Phil. from SISSA (Italy) in 1990 and his Ph.D. from ETH Zurich in 1993, under the supervision of Michele Parrinello. Since 1990, he has been using and developing first-principles methods for calculating the properties of molecules and condensed phases. He is a Reader at Queen's University Belfast, and in 2006, he published a textbook on Electronic Structure Calculations with Cambridge University Press.

Ruth Lynden-Bell received her Ph.D. degree from the University of Cambridge in 1962. She has been using atomistic simulation to study liquids, solutions, and other systems for many years. She moved to Queen's University from Cambridge in 1995, and returned to Cambridge as an emeritus professor in 2003, where she is still actively pursuing research into liquids and solutions.

Carlos Pinilla graduated in 2003 with a Licentiate in Physics from the Universidad Nacional de Colombia. He is currently a Ph.D. student at the Atomistic Simulation Centre where he works on the simulation of complex ionic systems. He focuses on the study of dynamical and structural properties of confined ionic liquids. He has also an interest in investigating the response of these systems to external perturbations as well as the use of ab initio methods to predict structural properties of their solid phase.
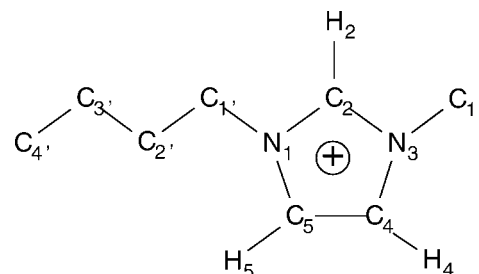
* Corresponding author. Tel: ++44 (2890) 975327. Fax: + 44 (2890) 241958. E-mail: m.del-popolo@qub.ac.uk.
† Queen's University Belfast.
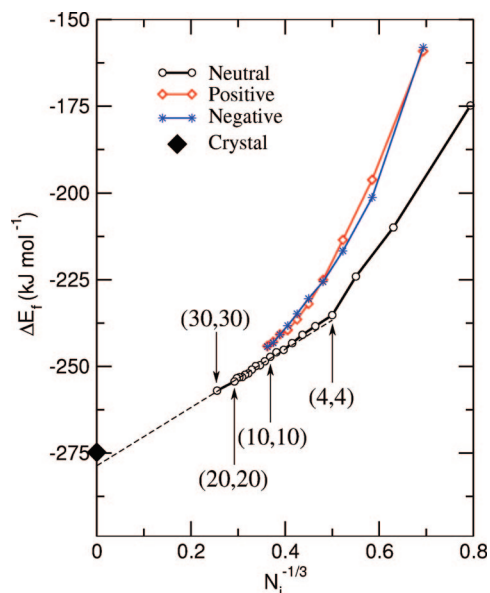‡ Cambridge University.

FIGURE 2. Cohesive energy per ion of neutral and singly charged [bmim][Tf] clusters as a function of $1/N^{1/3}$. N is the total number of ions in the cluster. The dashed line is a linear interpolation for the energy of neutral clusters larger than (12,12). The black diamond at the ordinate shows the energy of the crystal, computed with the force field used for the clusters. Reproduced with permission from ref 1. Copyright 2007 American Chemical Society.

Many properties of ionic liquids can be interpreted in terms of a balance between Coulomb and van der Waals forces, leading to the question of the accuracy of DFT calculations in describing the equilibrium density and volume dependence of structural parameters in these materials.[9] Such topics are discussed in section IV.

Finally, we consider the complexes that Brønsted acids form in molten salts. These are anionic complexes stabilized by strong hydrogen bonding between the proton-donor molecule and the ionic liquid anions.[10] The characterization of such complexes in terms of structure, relative stability, and vibrational frequencies is important to understand acid–base chemistry and proton transport in ionic liquids.

II. Clusters and Gas Phase Composition of a Room Temperature Molten Salt

We performed extensive calculations to optimize the structure and explore the thermal behavior of a series of charged and neutral clusters of 1-butyl-3-methylimidazolium trifluoromethylsulfonate ([bmim][Tf]).[1] The aggregates ranged from single isolated ions up to a nanodroplet of 30 ion pairs. Simulations were based on the force field of reference,[11] and involved both a fine-tuned simulated-annealing Monte Carlo algorithm and the basin hopping technique.[12]

Figure 2 shows the cohesive energy per ion for neutral and charged clusters as a function of $N^{-1/3}$. Here $N = n^+ + n^-$, and n^+ and n^- are the number of cations and anions, quoted as an ordered pair (n^+, n^-) in the following discussion. In the case of neutral clusters, the convergence to the cohesive energy of the crystal is remarkably smooth,
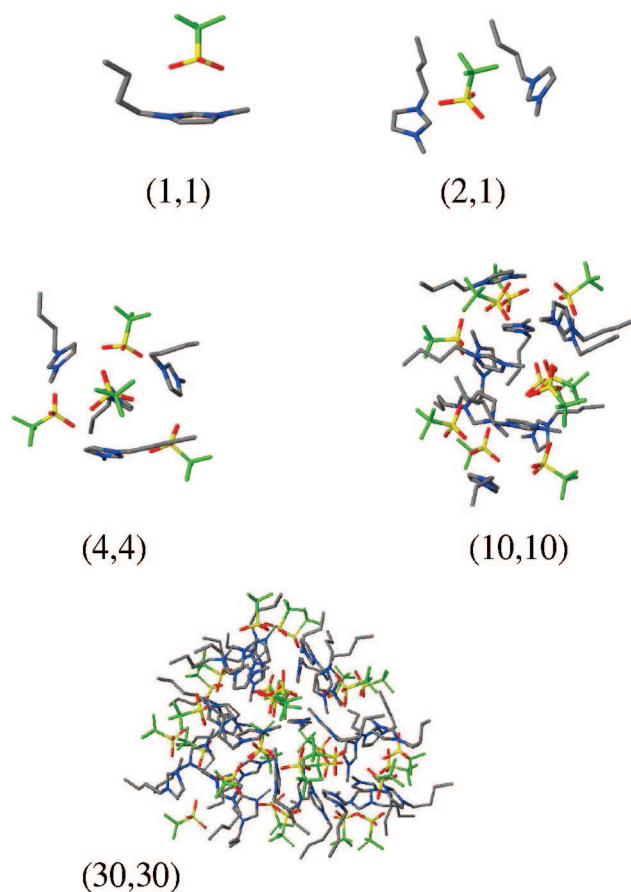

FIGURE 3. Lowest energy structure for selected neutral and charged clusters. The ordered pair (n^+, n^-) gives the number of cations and anions respectively. Reproduced with permission from ref 1. Copyright 2007 American Chemical Society.

and even for the smallest aggregates there are no signs of enhanced stability peaks or "magic numbers". Although the absence of favored sizes could be attributed to an incomplete optimization, we have argued that this effect is genuine, and it is associated with the intricate potential energy surface of ionic liquids.[1] Such complexity was attributed to the symmetry and flexibility of the cation that gives rise to a variety of local minima with very similar energies.

Figure 3 shows the lowest energy structures of a few clusters. The absence of strict ordering and symmetry is evident even for clusters as small as four ion pairs, (4,4). All the aggregates are spheroidal with either prolate or oblate form, and their surface is populated by both anions and cations. The butyl chain of bmim$^+$ and the sulfur–carbon axis of Tf$^-$ tend to align in the radial direction, while the imidazolium ring tends to orient tangential to the surface. The butyl tails show *trans/gauche* rotational conformers around the $C_1'-C_2'$ bond, with an 80% predominance of the *gauche* form. The presence of the two isomers in all the optimized structures is interesting, because only one of them (*gauche*) is eventually selected in the crystal. Such conformational freedom of the alkylimidazolium salts is behind the polymorphism observed in compounds such as [bmim][Cl] or [bmim][Br].[13,14]
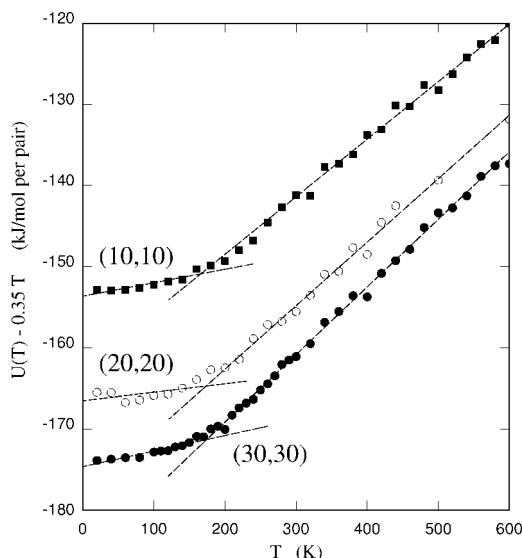
FIGURE 4. Average potential energy per ion pair U as a function of T for the (10,10), (20,20), and (30,30) clusters. In order to highlight the change of slope, a linear term $U_{lin} = 0.35T$ was subtracted from each curve. Reproduced with permission from ref 1. Copyright 2007 American Chemical Society.

We analyzed thermodynamic and dielectric properties of clusters as a function of temperature. Figure 4 shows the thermal evolution of the potential energy of some of the clusters. $U(T)$ shows low and high temperature linear regimes that intersect each other at $T \approx 180$ K. No discontinuity or anomaly is observed at the experimental melting point of [bmim][Tf], $T_m = 286$ K.[15] The transition between the two linear regimes is continuous and fairly marked, and the transition temperature increases slightly, but systematically, with system size. Based on the behavior of the different energy components, we have argued that this phase transition can be either a precursor of the bulk glass transition[15] ($T_g \approx 200$ K) or a weakly first-order transition corresponding to a defective crystallization.

Solidification is accompanied by a change in the dielectric properties of the cluster. As temperature decreases so does the average dipole length, $\langle |D| \rangle$, although at the lowest temperature the distribution of dipole lengths, $P(|D|)$, shows a dipole fluctuating around a small but non-negligible residual value. In the liquid range ($T_g \approx 250$ K), $P(|D|)$ is approximately Gaussian, and near the solidification point, it shows a clear change in the pattern of dipole fluctuations (see Figure 12 of ref 1). At this point, $P(|D|)$ is bimodal, suggesting the coexistence of a solid-like and a liquid domain. The first domain carries a permanent dipole moment, while the latter provides a background of Gaussian fluctuations.

Separating the Coulomb and van der Waals contributions to the energy difference between optimum structures provided a clear picture of the bonding in [bmim][Tf]. Starting with the isolated ions, $bmim^+$ and Tf^-, the formation of a single ion pair is dominated by electrostatic energy. Henceforth, the addition of neutral pairs to form larger clusters results in dispersion energy gains that increase substantially relative to the electrostatic gain. For large clusters, the addition of a new ion
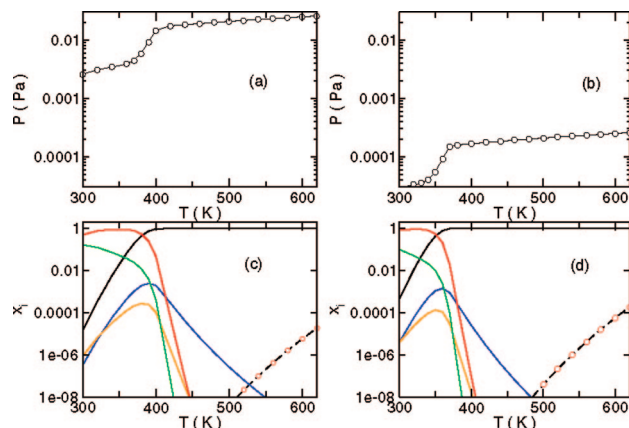

FIGURE 5. Total pressure as function of T at two different densities: (a) $\rho_1 = 10^{-5}$ mol/m^3; (b) $\rho_2 = 10^{-7}$ mol/m^3. Molar fraction of neutral and charged species in the gas phase at (c) $\rho_1 = 10^{-5}$ mol/m^3 and (d) $\rho_1 = 10^{-7}$ mol/m^3. In the lower panels, full curves are for neutral species: black (1,1); blue (2,2); orange (3,3); red (4,4), green (5,5). Dashed lines and symbols are for charged species: black dash line (1,0); red circles (0,1). Reproduced with permission from ref 1. Copyright 2007 American Chemical Society.

pair produces a change in dispersion energy of 75% that of the Coulomb counterpart. At variance with inorganic salts, both contributions have similar strength in RTILs. This balance between long- and short-range forces, associated with neutral and charged moieties in the ions, explains some structural patterns observed in crystals of alkylimidazolium salts (see Figure 8 and discussion in section IV).

Finally, we used the energies of Figure 2 to calculate the composition of the gas phase of [bmim][Tf].[4] The species present in the vapor result from the aggregation equilibrium between free ions, neutral ion pairs, and clusters of larger size. For a given temperature and density, the concentration of each component is found by solving the chemical equilibrium relations for a set of aggregation/deaggregation reactions in an ideal gas mixture (see section III-B of ref 1).

Panels a and b of Figure 5 show the relative concentration of species in the gas for two densities, $\rho_1 = 10^{-5}$ mol/m^3 and $\rho_2 = 10^{-7}$ mol/m^3. It is clear that large aggregates are favored at low temperature, being stabilized by a large cohesive energy gain. Of course, at low temperatures the vapor–liquid equilibrium is displaced toward the liquid and the absolute concentration of such clusters in the real vapor has to be very small. At high temperatures ($T > 400$ K), entropy favors fragmentation and the concentration of small clusters increases. Above 500 K, the single ion pair accounts for almost all the particles in the system, and at 600 K, which is the limit of thermal stability of [bmim][Tf], free ions appear in a small but non-negligible concentration. In conclusion, the concentration of the species in the gas phase results from the competition between potential energy and entropy, and the resulting speciation determines the shape of the pressure profiles in panels a and b of Figure 5.

III. Ab-initio simulation of a model ionic liquid

When we started this project, there was already a significant experience in describing room-temperature ionic liquids using empirical force fields, beginning with the seminal work of Hanke et al.[16] It was clear that such force fields were able to reproduce to a good extent a number of structural properties such as radial distribution functions, but their success was more limited in predicting three-dimensional distributions and features associated with quantum-mechanical interactions such as hydrogen bonding. In addition, the procedure used to extract real-space structural information from reciprocal-space neutron data, namely, the EPRS method of A. Soper,[17] was being pushed to another level of complexity by moving from relatively simple molecular liquids, for example, water, into the significantly more complex imidazolium salts.[18] Such circumstances suggested that it was important to validate both approaches by means of a more fundamental computational method. We then decided to undertake what would be the first ab initio molecular dynamics simulation of a room-temperature molten salt,[5] that was closely followed by the work of other groups arriving to similar conclusions.[19,20]

We performed an extensive study of dimethylimidazolium chloride ([mmim][Cl]) using the SIESTA DFT code.[21] The reliability of this approach was tested on the solid phase and the isolated ion pair. In the first case, starting from the experimental crystal structure, the atomic positions were optimized within a unit cell constrained to the experimental shape and volume. The resulting intra and intermolecular distances and angles were in very good agreement with the experimental ones, and therefore, the liquid phase was simulated at constant volume in conformance with the experimental density. In light of the results presented in section IV, this is a constraint that compensates for the lack of cohesion associated with the DFT approach used in our work (PBE-GGA). Its potential effect on structural properties other than the density should be kept in mind.

A very important issue in the case of ionic liquids is that their dynamics is very slow.[22] Therefore, a reliable statistical sampling of the liquid cannot be obtained by running a single very long trajectory. It proved much better to average several trajectories starting from different initial conditions. This also provided a way of introducing error bars and helped detecting unreliable features due to insufficient statistical sampling.

In Figure 6, we show the site–site radial distributions for the Cl⁻ anion with respect to the atoms in the imidazolium ring and also the ring hydrogens. The peaks of the distributions correspond quite well with the contacts in the solid phase (shown by arrows) and appear at considerably shorter distances than those obtained from simulations with empirical models. Comparison with the isolated ion pair is not straightforward because our lowest-energy structure had the Cl⁻ above the plane of the ring, in a configuration quite different from that assumed in
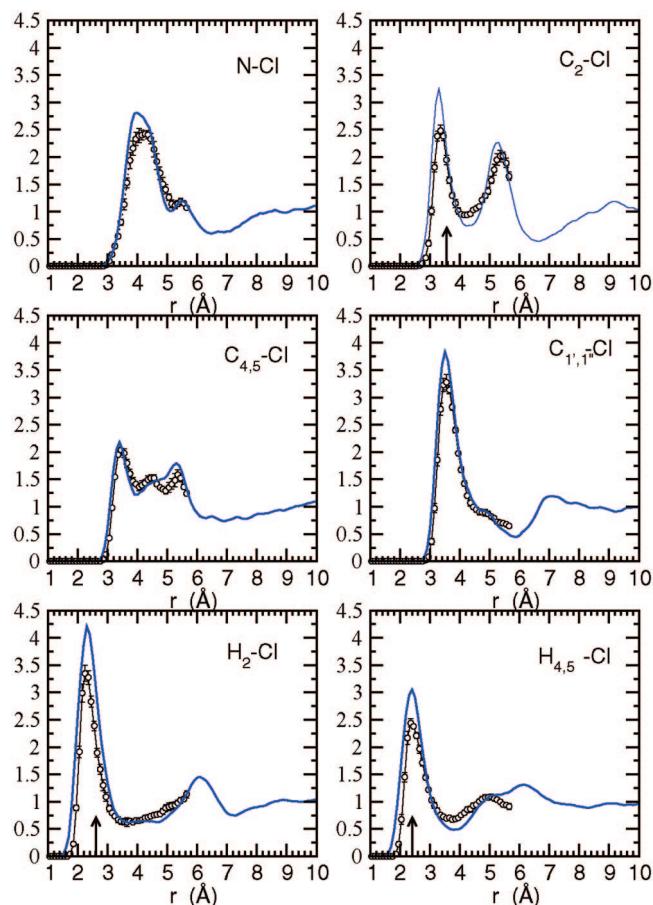

FIGURE 6. Site–site radial distribution functions, $g_{ab}(r)$, between different cation atoms and chloride. Lines with circles and solid blue lines correspond to systems of 8 and 24 ion pairs, respectively. Simulations were run at the experimental density of [mmim][Cl] at 450 K. The arrows represent the corresponding contacts in the solid phase. Atom labeling can be inferred from Figure 1. Reproduced with permission from ref 5. Copyright 2005 American Chemical Society.

the liquid. We also found another local minimum with a similar energy and more reminiscent of the liquid structure (see Figure 2 in ref 5), but the finite temperature study was reported only for the former.

A more stringent test is the three-dimensional distribution of anions around the cation's center. In Figure 7, we show such distribution from our ab initio simulations, where it can be seen that the Cl⁻ anions are coordinated with the ring hydrogens. Moreover, each anion appears to be coordinated with hydrogens in three cations, all at distances smaller than 3.5 Å, and the H···Cl bonds turn out to be quite directional. This, together with experimental evidence,[18] suggested the formation of C–H···Cl hydrogen bonds. We analyzed this possibility by computing the Cl⁻ distributions around the C–H bond axis (Figure 10 in ref 5) and found that typical bond lengths and angles did indeed correspond to moderate hydrogen bonds. The H···Cl distance was too long to involve chemical bonding, but electronic polarization effects could be important to describe these specific interactions.

We subsequently confirmed this observation by studying the distribution of molecular dipole moments
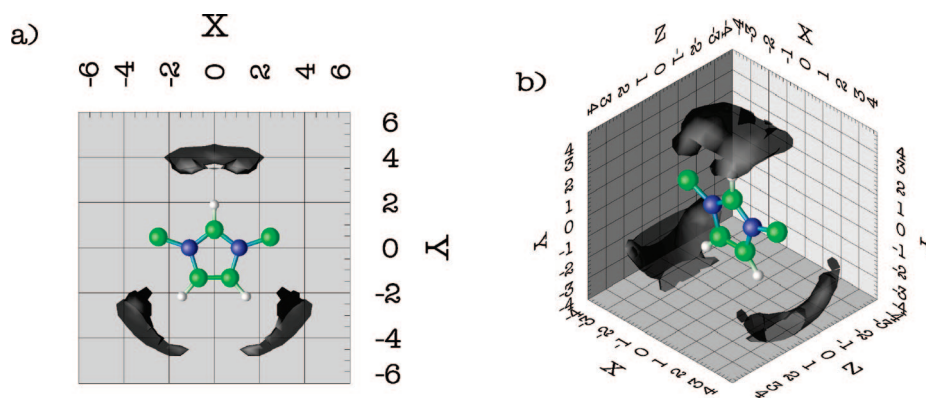
FIGURE 7. Probability distribution of Cl^- around $mmim^+$. The isosurface corresponds to a density level of 0.03 Å^{-3}, which is 6 times the average number density of anions. Methyl hydrogens have been omitted from the molecular model. *X, Y, Z* coordinates in angstroms. Reproduced with permission from ref 5. Copyright 2005 American Chemical Society.
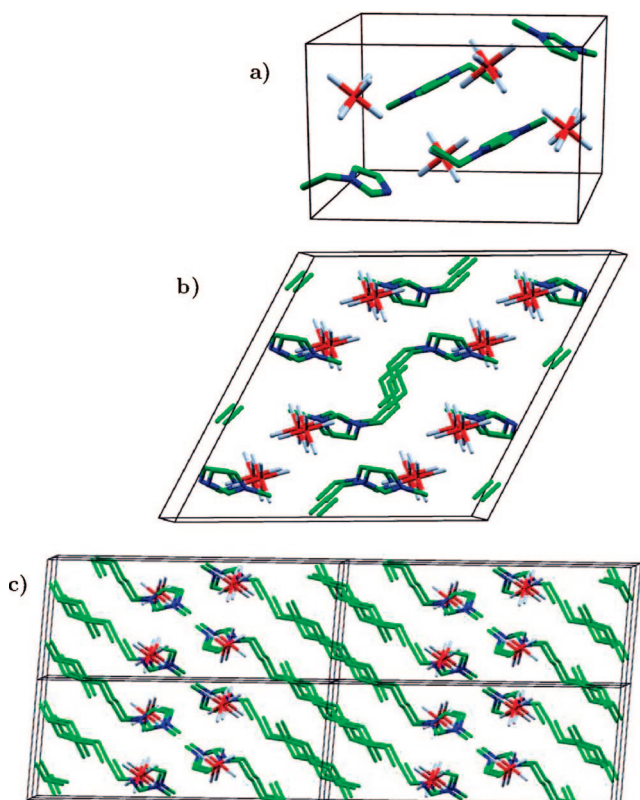

FIGURE 8. Crystal structure of (a) [emim][PF_6], (b) [bmim][PF_6], and (c) [ddmim][PF_6]. Note the arrangement of the alkyl chains.

FIGURE 9. (a) Joint probability distribution $P(l_1, l_2)$, for the two hydrogen–chlorine bond lengths, l_1 and l_2, in $ClHCl^-$ and (b) distribution of bending angles, $P(\alpha)$. Reproduced with permission from ref 10. Copyright 2006 American Chemical Society.

($|\mu|$) in the liquid phase.[6] In the case of $mmim^+$, the origin was set at the geometric center of the imidazolium ring. The most likely value of $|\mu|$ for the cations in the liquid phase was about 0.7 D larger than that of an isolated cation at the same temperature and, accordingly, larger than that calculated with most fixed-charge models. In addition, we observed a sizable dipole moment in the Cl^- anion, which was purely due to polarization. Both dipole moment distributions exhibited significant fluctuations. In the case of cations, such fluctuations (see Figure 1 of Lynden-Bell's paper in this issue) are equally shared by thermal and electronic polarization effects. Experience has shown, however,

that polar molecules can be modeled satisfactorily with nonpolarizable models, if the charges are chosen to produce an enhanced dipole moment. We did this by constructing a nonpolarizable flexible model that reproduced the forces calculated in the ab initio MD simulation,[23] obtaining radial and angular distributions in better agreement with ab initio distributions than other force fields of the same functional form.

Table 1. Zero-Pressure Equilibrium Volume (Å³) of the RTIL Crystals[a]

comp	[mmim][PF$_6$]	[emim][PF$_6$]	[bmim][PF$_6$]	[ddmim][PF$_6$]	[bmim][Cl]-I	[bmim][Cl]-II	[mmim][Cl]
exp	1893.9	1023.9	605.0	2000.6	961.2	966.7	687.6
ref	26	27	28	29	13	13	30
T [K]	173	102	173	123	173	173	203
Z	8	4	2	8	4	4	4
extrapol	1840.3	1014.1	590.4	1962.5	947.3	948.1	674.5
LDA	1628.9	892.1	520.9	1710.9	843.9	836.7	596.6
	(−11.5)	(−12.0)	(−11.8)	(−12.8)	(−10.8)	(−11.7)	(−11.5)
GGA	2038.4	1120.4	650.0	2258.0	1036.6	1051.3	742.8
	(10.8)	(10.5)	(10.1)	(15.1)	(9.4)	(10.9)	(10.1)
FFM	1837.9	1010.6	609.5	1947.3	936.9	952.6	682.2
	(1.8)	(−0.3)	(3.2)	(−0.8)	(−1.1)	(0.5)	(1.1)

[a] The lines below the name of the compounds report the raw experimental numbers (exp), the reference (ref) providing the experimental unit cell parameters and relative atomic coordinates, the temperature (T) of the sample, the number of neutral ion pairs in the unit cell (Z), and the experimental volume extrapolated to the limit of $T = 0$ and classical ions (extrapol), followed by the computational results. Relative errors (in percent) are reported in parentheses following the computational result. Table and caption reproduced with permission from ref 9. Copyright 2007 American Institute of Physics.

IV. Electronic Structure Calculations for Crystals of Alkyl-Imidazolium Salts

In sections III and V of this paper, we discussed DFT-based simulations of ionic liquids in which the density of the system was fixed to the experimental value. Given the limitations of standard DFT schemes in reproducing the attractive tail of van der Waals interactions, it was important to assess their accuracy when describing the volumetric properties of RTILs. As organic ionic compounds, these materials are halfway between ionic systems (where standard DFT performance is fairly good) and systems containing weakly interacting components (for example, noble gases and nonpolar molecules, where these calculations are problematic).[7,8]

Starting with the experimental crystal structure, we performed a long series of geometry optimizations using the local[24] (LDA) and one semilocal approximation[25] (PBE-GGA) to DFT, as implemented in the SIESTA code.[21] In order to subtract thermal and quantum effects from the experimental volumes, and thus allow for a better comparison with theoretical results, we resorted to the quasi-harmonic approximation (QHA). The same calculations were performed with the empirical force field (FF) of ref 11. The final result was a complete picture in which DFT, FF, and experimental data can be compared.[9]

Computations were performed on (i) a sequence of [R-mim][PF$_6$] salts, where R represents methyl ([mmim][PF$_6$]), ethyl ([emim][PF$_6$]), butyl ([bmim][PF$_6$]), and dodecyl ([ddmim][PF$_6$]) groups and (ii) two chloride salts, [mmim][Cl] and [bmim][Cl]. From the first series, one can assess the performance of DFT since the role of van der Waals interactions is enhanced due to the growth of the alkyl tail at fixed anion. On the other side, effects associated with changes in Coulomb energy can be assessed from the comparison of compounds with the same cation but different anions ([mmim][PF$_6$]/[mmim][Cl] and [bmim][PF$_6$]/[bmim][Cl]). The experimental crystallographic structures of some PF$_6$ salts are shown in Figure 8, where a clear arrangement of ionic and nonionic domains is observed as the alkyl tail grows.

Table 1 reports the equilibrium volumes predicted by LDA, PBE-GGA, and FF. The first striking result is the 20% difference between the volumes predicted by LDA and PBE-GGA, pointing to a problem with the intermolecular interactions. In contrast, the volumes calculated with the force field agree with the experimental data within a maximum error of 3%. The removal of quantum and thermal expansion contributions to the experimental volume ($T \neq 0$ K) results in a contraction of around 2% for all the systems, thus allowing for a cleaner comparison with the DFT calculations ($T = 0$ K).

The two DFT approximations incur a significant error as evidenced by the underestimation and overestimation of the experimental volume by LDA and PBE-GGA, respectively. The relative error of PBE-GGA is practically the same for [mmim][PF$_6$], [emim][PF$_6$] and [bmim][PF$_6$] but increases significantly for [ddmim][PF$_6$], where the hydrocarbon chain is longer. The relative error of LDA is around 10% across the whole series. The results for the chloride crystals exhibit similar trends and show little effect from the change of anion. The intramolecular structure of the ions is well described by both approximations, with the most affected parameters being the P–F covalent bonds. Some of these bonds stretched up to 5% with respect to the experimental bond length.

Intermolecular distances are far more sensitive to the choice of exchange and correlation functional. By looking at the changes in close-contact distances, it became clear that (i) PBE-GGA overestimates distances where LDA underestimates them and (ii) the PBE-GGA error increases with the size of the lateral chain while LDA errors do not show a clear trend. We also verified that fixing the cell parameters to the experimental values and optimizing the atomic positions resulted in a good description of the equilibrium atomic coordinates. This suggests that standard DFT schemes can be safely used for RTILs provided that the volume of the system is fixed to the correct value. Unfortunately, this approach is impractical for inhomogeneous systems such as clusters and interfaces.

The trends observed in equilibrium volume and atomic positions manifest themselves also in the cohesive energy of the crystals, E_{coh}, reported in Table 2. The difference in E_{coh} between LDA and PBE-GGA is very large (around 1 eV per ion pair) and increases with the length of the

Table 2. Computed cohesive energy (in eV per neutral ion pair) of alkyl-imidazolium crystals.[a]

	LDA	GGA	FFM
[mmim][PF_6]	2.372	1.637	2.257
[emim][PF_6]	2.420	1.546	2.296
[bmim][PF_6]	2.480	1.445	2.237
[ddmim][PF_6]	3.113	1.510	2.803
[nmim][Cl]	2.258	1.478	2.392
[bmim][Cl]-I	2.252	1.2855	2.480
[bmim][Cl]-II	2.308	1.349	2.401

[a] E_{coh} is defined with respect to the energy of the gas-phase neutral ion pair. Reproduced with permission from ref 9. Copyright 2007 American Institute of Physics.

alkyl tail. LDA cohesive energies are remarkably close to those obtained with the force field, owing to a fortuitous compensation of errors.

The rationalization of the former results was extensively discussed in ref 9 and can be summarized as follows: both local and semilocal approximations to DFT misrepresent dispersion interactions. This is the main source of error on PBE-GGA, at least as concerns cohesion and volumetric properties. In the case of LDA, the former effect is overcompensated by a spurious attraction between slightly overlapping closed-shell fragments, thus resulting in a higher equilibrium density.

V. The State of the Proton in Ionic Liquids

Ionic liquids have been extensively investigated as solvents for chemical reactions and as electrolytes for electrochemical devices. In this last sense, it is worth mentioning their potential application as proton conductors in fuel cells.[31,32] Proton transport capacity and acid–base chemistry in molten salts have the microscopic behavior of protons in solution as a common factor.

In ref 10, we considered the addition of a Brønsted acid molecule to a molten salt, specifically HCl in [mmim][Cl], with the aim of understanding the energetics and solvation structure of the acidic proton, as well as the transport mechanism of such protons through the solvent. Since in this case the breaking and formation of chemical bonds is a central issue, we resorted again to ab initio MD simulations with SIESTA.[21] We observed that the HCl molecule in [mmim][Cl] immediately binds to a Cl^- ion forming a $ClHCl^-$ molecule. This species is an example of a more general class of complexes of the type AHB^-, in which the proton-donor molecule binds to an anion in solution. In our case, A and B (i.e., the molecules that flank the proton) correspond to Cl and Cl^-, but they can be replaced by other anions like NO_3^-, BF_4^-, PF_6^-, SO_4H^-, etc. In the gas phase, such complexes exist as rather strongly bound species, and in the case of halogens, they are known to be symmetric, and their stability is known to decrease from F^- toward I^-.[33–35] The question arises as to whether this geometry is retained in the ionic liquid. Figure 9a shows a contour plot of the joint probability distribution of the two bond lengths in $ClHCl^-$, where a single maximum indicates that the proton is symmetrically located at 1.55 Å from each Cl atom. The
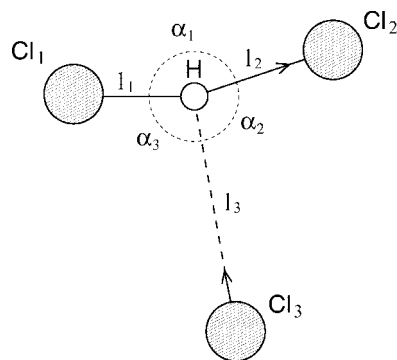

FIGURE 10. The old molecule is $Cl_1HCl_2^-$. Cl_3 enters and displaces Cl_2 forming a new molecule $Cl_1HCl_3^-$. ζ_1 is defined as $l_1 - l_2$. Note that if a distortion with negative ζ_1 occurs then Cl_1 and Cl_2 change roles. Reproduced with permission from ref 10. Copyright 2006 American Chemical Society.

geometry of the complex is barely modified from that of the gas phase, at variance with observations in some ionic crystals.[36–38] That the anion remains linear is seen in Figure 9b, which shows the distribution of bending angles peaking at 180°. For the solvation shell of this species, we observed a strong correlation between the asymmetric stretching and the coordination of each chlorine with the hydrogen atoms in the cations. The Cl^- that moves away from the central hydrogen acquires a larger charge thus gaining coordination.

We then studied the proton exchange reaction depicted in Figure 10, where a third Cl^- enters the sphere of the $ClHCl^-$ complex making a bond with the acidic proton and displacing one of the two other chloride anions. This process suggests a possible proton hopping mechanism that might compete with the diffusion of $ClHCl^-$ as a whole. Whether one or the other mechanism is favored depends on their relative activation barriers and on thermodynamic conditions. For the hopping mechanism, we estimated a quite large free energy barrier of about 0.4 eV. The structural rearrangments associated with this process can be described in the following way: when $ClHCl^-$ is asymmetrically stretched, a third Cl^- anion approaches the proton perpendicular to the axis of the molecule forming a highly asymmetric Cl_3H^{-2} complex. As detailed in ref 10, the formation of this complex is the kinetic bottleneck of the reaction. The process ends with the ejection of the asymmetrically stretched Cl^- leading to a new $ClHCl^-$ molecule.

VI. Summary

An extensive study of [bmim][Tf] clusters revealed a number of interesting features such as the absence of magic numbers and the hint of a phase transition that is accompanied by a peculiar change of dielectric behavior. A chemical thermodynamical study showed that at temperatures close to the upper stability limit of [bmim][Tf] the vapor phase is made of neutral ion pairs with small amounts of free ions.

We have used ab initio calculations and molecular dynamics simulations to understand the structural properties of liquids and crystals of dialkylimidazolium

salts. The correct picture unveils a complex scenario where a balance between Coulomb, van der Waals, and sometimes moderate hydrogen-bonding interactions, determines the macroscopic properties and behavior of RTILs. Such balance is crucial when describing structures of reduced dimensionality such as surfaces, interfaces, and clusters.

By comparing local (LDA) and semilocal (PBE-GGA) density functional calculations with empirical force fields and experimental data, we have found that the equilibrium volume predicted by either approximation is affected by significant errors of similar magnitude but of opposite sign. However, optimization of atomic positions within the experimental unit cell provides results in good agreement with the experimental structures.

We have started to address the central issue of chemical reactivity in ionic liquids by focusing on acid–base processes. We have shown that Brønsted acids in ionic liquids form strongly hydrogen-bonded anions whose relative stability determines acid–base behavior and affects proton transport capacity.

References

(1) Ballone, P.; Pinilla, C.; Kohanoff, J.; Del Pópolo, M. Neutral and Charged 1-Butyl-3-methylimidazolium Triflate Clusters: Equilibrium Concentration in the Vapor Phase and Thermal Properties of Nanometric Droplets. *J. Phys. Chem. B* **2007**, *111*, 4938–4950.

(2) Fenn, J. B.; Mann, M.; Meng, C. K.; Wong, S. F.; Whitehouse, C. Electrospray Ionization for Mass-Spectroscopy of Large Biomolecules. *Science* **1989**, *246*, 64–71.

(3) Martin, T. P. Alkali-Halide Clusters and Microcrystals. *Phys. Rep.* **1983**, *95*, 167–199.

(4) Earle, M. J.; Esperanca, J. M. S. S; Gilea, M. A.; Canongia Lopes, J. N.; Rebelo, L.P.N; Magee, J. W.; Seddon, K. R.; Widegren, J. A. The Distillation and Volatility of Ionic Liquids. *Nature* **2006**, *439*, 831–834.

(5) Del Pópolo, M. G.; Lynden-Bell, R. M.; Kohanoff, J. Ab Initio Molecular Dynamics Simulation of a Room Temperature Ionic Liquid. *J. Phys. Chem. B* **2005**, *109*, 5895–5902.

(6) Resende Prado, C. E.; Del Pópolo, M. G.; Youngs, T. G. A.; Kohanoff, J.; Lynden-Bell, R. M. Molecular Electrostatic Properties of Ions in an Ionic Liquid. *Mol. Phys.* **2006**, *104*, 2477–2483.

(7) Kristyán, S.; Pulay, P. Can (Semi)Local Density-Functional Theory Account for the London Dispersion Forces. *Chem. Phys. Lett.* **1994**, *229*, 175–180.

(8) Meijer, E. J.; Sprik, M. A Density-Functional Study of the Intermolecular Interactions of Benzene. *J. Chem. Phys.* **1996**, *105*, 8684–8689.

(9) Del Pópolo, M. G.; Pinilla, C. ; Ballone, P. Local and Semi-Local Density Functional Computations for Crystals of 1-Alkyl-3-methylimidazolium Salts. *J. Chem. Phys.* **2007**, *126*, 144705.

(10) Del Pópolo, M. G.; Kohanoff, J.; Lynden-Bell, R. M. Solvation Structure and Transport of Acidic Protons in Ionic Liquids: A First-principles Simulation Study. *J. Phys. Chem B* **2006**, *110*, 8798–8803.

(11) (a) Canongia Lopes, J. N.; Deschamps, J.; Padua, A. A. H. Modeling Ionic Liquids Using a Systematic All-Atom Force Field. *J. Phys. Chem. B.* **2004**, *108*, 2038–2047. (b) Canongia Lopes, J. N.; Padua, A. A. H. Molecular Force Field for Ionic Liquids Composed of Triflate or Bistriflylimide Anions. *J. Phys. Chem. B* **2004**, *108*, 16893–16898. See also Canongia Lopes, J. N.; Deschamps, J. ; Padua, A. A. H. Correction to Modeling Ionic Liquids Using a Systematic All-Atom Force Field. *J. Phys. Chem. B* **2004**, *108*, 11250.

(12) Wales, D. J.; Doye, J. P. K. Global Optimization by Basin-Hopping and the Lowest Energy Structures of Lennard-Jones Clusters Containing up to 110 Atoms. *J. Phys. Chem. A* **1997**, *101*, 5111–5116.

(13) Holbrey, J. D.; Reichert, W. M.; Nieuwenhuyzen, M.; Johnston, S.; Seddon, K. R.; Rogers, R. D. Crystal Polymorphism in 1-Butyl-3-methylimidazolium Halides: Supporting Ionic Liquid Formation by Inhibition of Crystallization. *Chem. Commun.* **2003**, *14*, 1636–1637.

(14) (a) Hayashi, S.; Ozawa, R.; Hamaguchi, H. Raman Spectra, Crystal Polymorphism, and Structure of a Prototype Ionic-Liquid [bmim]Cl. *Chem. Lett.* **2003**, *32*, 498–499. (b) Saha, S.; Hayashi, S.; Kobayashi, A.; Hamaguchi, H. Crystal Structure of 1-Butyl-3-methylimidazolium Chloride. A Clue to the Elucidation of the Ionic Liquid Structure. *Chem. Lett.* **2003**, *32*, 740–741. (c) Hamaguchi, H.-O.; Ozawa, R. *Adv. Chem. Phys.* **2005**, *131*, 85.

(15) Fredlake, C. P.; Crosthwaite, J. M.; Hert, D. G.; Aki, S. N. V. K.; Brennecke, J. F. Thermophysical Properties of Imidazolium-Based Ionic Liquids. *J. Chem. Eng. Data* **2004**, *49*, 954–964.

(16) Hanke, C. G.; Price, S. L.; Lynden-Bell, R. M. Intermolecular Potentials for Simulations of Ionic Liquids. *Mol. Phys.* **2001**, *99*, 801–809.

(17) Soper, A. K. Empirical Potential Monte Carlo Simulation of Fluids Structure. *Chem. Phys.* **1996**, *202*, 295–306.

(18) Hardacre, C.; Holbray, J. D.; McMath, S. E. J.; Bowron, D. T.; Soper, A. K. Structure of Molten 1,3-Dimethylimidazolium Chloride Using Neutron Difraction. *J. Chem. Phys.* **2003**, *118*, 273–278.

(19) Buhl, M.; Chaumont, A.; Schurhammer, R.; Wipff, G. Ab Initio Molecular Dynamics of Liquid 1,3-Dimethylimidazolium Chloride. *J. Phys. Chem. B* **2005**, *109*, 18591–18599.

(20) Bhagarva, B. L.; Balasubramanian, S. Intermolecular Structure and Dynamics in an Ionic Liquid: A Car–Parrinello Molecular Dynamics Simulation Study of 1,3-Dimethylimidazolium Chloride. *Chem. Phys. Lett.* **2006**, *417*, 486–491.

(21) Soler, J. M.; Artacho, E.; Gale, J.; García, A.; Junquera, J.; Ordejón, P.; Sánchez-Portal, D. The Siesta Method for Ab Initio Order-N Materials Simulation. *J. Phys.: Condens. Matter* **2002**, *14*, 2745–2779.

(22) Del Pópolo, M. G.; Voth, G. A. On the Structure and Dynamics of Ionic Liquids. *J. Phys. Chem. B* **2004**, *108*, 1744–1752.

(23) Youngs, T. G. A.; Del Pópolo, M. G.; Kohanoff, J. Development of Complex Classical Force Fields through Force Matching to ab Initio Data: Application to a Room-Temperature Ionic Liquid. *J. Phys. Chem. B* **2006**, *110*, 5697–5707.

(24) Hohenberg, P.; Kohn, W. Inhomogeneous Electron Gas. *Phys. Rev.* **1964**, *136*, B864–B871.

(25) Perdew, J. P.; Burke, K. ; Ernzerhof, M. Generalized Gradient Approximation Made Simple. *Phys. Rev. Lett.* **1997**, *77*, 3865–3868; **1997**, *78* 1396 (erratum).

(26) Holbrey, J. D.; Reichert, W. M.; Nieuwenhuyzen, M.; Sheppard, O.; Hardacre, C.; Rogers, R. D. Liquid Clathrate Formation in Ionic Liquid-Aromatic Mixtures. *Chem. Commun.* **2003**, *4*, 476–477.

(27) Barker, B.L. ; Stanley, G. G. ; Fronczek, F. R.; Cambridge Crystallographic Data Centre Private Communication; 2004; Deposition Number 228745.

(28) (a) Dibrov, S. M.; Kochi, J. K. Crystallographic view of fluidic structures for room-temperature ionic liquids: 1-butyl-3-methylimidazolium hexafluorophosphate. *Acta Crystallogr.* **2006**, *C62*, o19. A very similar structure (measured at $T = 180$ K) is reported in: (b) Choudhury, A. R.; Winterton, N.; Steiner, A.; Cooper, A. I.; Johnson, K. A. In Situ Crystallization of Low-Melting Ionic Liquids. *J. Am. Chem. Soc.* **2005**, *127*, 16792–16793.

(29) Gordon, C. M.; Holbrey, J. D.; Kennedy, A.; Seddon, K. R. Ionic Liquid Crystals: Hexafluorophosphate Salts. *J. Mater. Chem.* **1998**, *8*, 2627–2636.

(30) Arduengo, A. J.; Rasika Dias, H. V.; Harlow, R. L.; Kline, M. Electronic Stabilization of Nucleophilic Carbenes. *J. Am. Chem. Soc.* **1992**, *114*, 5530–5534.

(31) Noda, A. ; Susan, A. B.; Kudo, K.; Mitsushima, S.; Hayamizu, K.; Watanabe, M. Bronsted Acid-Base Ionic Liquids as Proton-Conducting Nonaqueous Electrolytes. *J. Phys. Chem. B* **2003**, *107*, 4024–4033.

(32) Xu, W.; Angell, C. A. Solvent-Free Electrolytes with Aqueous Solution-Like Conductivities. *Science* **2003**, *302*, 422–425.

(33) Kawaguchi, K. Gas-Phase Infrared-Spectroscopy of ClHCl⁻. *J. Chem. Phys.* **1988**, *88*, 4186–4189.

(34) Thomson, C.; Clark, D. T.; Waddington, T. C.; Jenkins, H. D. B. Theoretical Studies on Hydrogen Dichloride, HCl_2^- Ion and Radical HCl_2. *J. Chem. Soc., Faraday Trans.* **1975**, *2*, 1942–1947.

(35) Del Bene, J. E.; Jordan, M. J. A Comparative Study of Vibrational Anharmonicity in the Bihalide Anions XHX⁻, X = F, Cl, Br. *Spectrochim. Acta, Part A* **1999**, *55*, 719–729.

(36) Ludman, C. J.; Waddington, T. C.; Salthouse, J. A.; Lynch, R. J.; Smith, J. A. S. Nuclear Quadrupolar Resonance and Structure of the Dichloride, HCl_2^-, Ion. *Chem. Commun.* **1970**, *227*, 405.

(37) Emsley, J. Very Strong Hydrogen Bonding. *Chem. Soc. Rev.* **1980**, *1*, 91–124.

(38) Pimentel, G. C.; McClellan, A. L. Hydrogen Bonding. *Annu. Rev. Phys. Chem.* **1971**, *22*, 347–385.

AR700069C